DISCLAIMER

This report was prepared as an account of work sponsored by an agency of the United States Government. Neither the United States Government nor any agency thereof, nor any of their employees, makes any warranty, express or implied, or assumes any legal liability or responsibility for the accuracy, completeness, or usefulness of any information, apparatus, product, or process disclosed, or represents that its use would not infringe privately owned rights. Reference herein to any specific commercial product, process, or service by trade name, trademark, manufacturer, or otherwise does not necessarily constitute or imply its endorsement, recommendation, or favoring by the United States Government or any agency thereof. The views and opinions of authors expressed herein do not necessarily state or reflect those of the United States Government or any agency thereof. Reference herein to any social initiative (including but not limited to Diversity, Equity, and Inclusion (DEI); Community Benefits Plans (CBP); Justice 40; etc.) is made by the Author independent of any current requirement by the United States Government and does not constitute or imply endorsement, recommendation, or support by the United States Government or any agency thereof.

Bypassing Fast Time Scales of the Hodgkin-Huxley Neuron Model via a Thresholded Hard Reset

Kevin Patrick Griffin, Kantapat Jungpaibul, M. Brooks Tellekamp, and Peter Graf

National Renewable Energy Laboratory

NREL is a national laboratory of the U.S. Department of Energy
Office of Energy Efficiency & Renewable Energy
Operated under Contract No. DE-AC36-08GO28308

This report is available at no cost from NREL at www.nrel.gov/publications.

Technical Report
NREL/TP-2C00-94669
November 2025

Bypassing Fast Time Scales of the Hodgkin-Huxley Neuron Model via a Thresholded Hard Reset

Kevin Patrick Griffin, Kantapat Jungpaibul, M. Brooks Tellekamp, and Peter Graf

National Renewable Energy Laboratory

Suggested Citation
Griffin, Kevin Patrick, Kantapat Jungpaibul, M. Brooks Tellekamp, and Peter Graf. 2025. *Bypassing Fast Time Scales of the Hodgkin-Huxley Neuron Model via a Thresholded Hard Reset*. Golden, CO: NREL. NREL/TP-2C00-94669. https://www.nrel.gov/docs/fy26osti/94669.pdf.

NREL is a national laboratory of the U.S. Department of Energy
Office of Energy Efficiency & Renewable Energy
Operated under Contract No. DE-AC36-08GO28308

This report is available at no cost from NREL at www.nrel.gov/publications.

Technical Report
NREL/TP-2C00-94669
November 2025

15013 Denver West Parkway
Golden, CO 80401
303-275-3000 • www.nrel.gov

NOTICE

This work was authored by NREL for the U.S. Department of Energy (DOE), operated under Contract No. DE-AC36-08GO28308. Funding provided by the Laboratory Directed Research and Development (LDRD) Program at NREL. The views expressed herein do not necessarily represent the views of the DOE or the U.S. Government.

This report is available at no cost from NREL at www.nrel.gov/publications.

U.S. Department of Energy (DOE) reports produced after 1991 and a growing number of pre-1991 documents are available free via www.OSTI.gov.

Cover photos (clockwise from left): Josh Bauer, NREL 61725; Visualization from the NREL Insight Center; Getty-181828180; Agata Bogucka, NREL 91683; Dennis Schroeder, NREL 51331; Werner Slocum, NREL 67842.

NREL prints on paper that contains recycled content.

Executive Summary

We propose a modification to the Hodgkin-Huxley model to reduce the numerical stiffness of the equations by introducing an explicit voltage threshold. When this threshold is crossed, the voltage and the gating variables are reset to constant values. It is found that, for all of the current stimuli considered, the proposed model accurately reproduces the behavior of the baseline Hodgkin-Huxley model while bypassing the fast dynamics of spiking. Specifically, the model accurately reproduces the spike times and, between spikes, the time courses of the membrane potential and gating variables.

Acknowledgments

This work was authored by the National Renewable Energy Laboratory (NREL) for the U.S. Department of Energy (DOE) under Contract No. DE-AC36-08GO28308. Funding provided by the Laboratory Directed Research and Development (LDRD) Program at NREL. The views expressed in the article do not necessarily represent the views of the DOE or the U.S. Government. Generative AI was used to support software development.

Table of Contents

List of Figures

1 Introduction

The Hodgkin-Huxley (HH) model is a biophysically inspired model that can capture a vast array of observed spiking behaviors of biological neurons upon calibration of the model's coefficients E. Izhikevich 2004. This suggests that the HH model could be used as a data-driven model for various types of biological neurons and biophysically realistic neuron devices. Large spiking neural networks of these neuron models could provide insights about the impact of neuron behavior on system-level dynamics in brains or biophysically realistic neuromorphic computers and accelerators.

However, the HH model is often thought to be too computationally expensive for use in large simulations since integrating it involves about 240 times as many floating point operations (flops) as the integrate and fire model E. Izhikevich 2004. Models that can also reproduce complex neuron spiking phenomena but with significantly fewer flops have been proposed such as the Izhikevich (Izh) model E. M. Izhikevich 2003, albeit with diminished biophysical interpretability.

In the modern era of high-performance computing, flop counting is no longer the focus due to the widespread use of parallel computing and advances in CPU and GPU technology. This implies that, today, perhaps the biggest drawback with using spike resolving models such as the HH or Izh models is that fast timescales associated with spike initiation lead to numerical stiffness, i.e., the need to take small time steps to resolve fast timescales. Implicit integration schemes can ensure stability but not accuracy. Adaptive time stepping enables larger time steps between spiking events. However, in simulations of larger networks, the odds increase that, at any point in time, at least one neuron is in a spiking state and requires a small time step thus eroding the savings from adaptive time stepping. Most importantly, the computational cost associated with time step restrictions typically cannot be diminished with additional computational resources since simulations typically cannot be parallelized in time.

One potential solution to this problem is the use of the quasi-steady-state approximation (QSSA) to bypass the time scale of the fast sodium activation gate m in the HH model Hodgkin and Huxley 1952. The QSSA approach replaces the ordinary differential equation (ODE) for the m variable with a voltage-dependent steady-state value $m_\infty(V_m)$. As will be shown, this approach results in a model that does not quantitatively recover the behavior of the HH model and does not decrease the fast changes in membrane potential with respect to time.

This motivates the present work, which aims to reduce the numerical stiffness of the HH equation system by bypassing the fast time scale of the sodium activation gate with an explicit voltage threshold and reset of the voltage and gating variables.

2 Model

The Hodgkin-Huxley (HH) model Hodgkin and Huxley 1952 describes membrane potential dynamics via

$$C_m \frac{dV_m}{dt} = I_{\text{ext}} - I_{\text{Na}} - I_{\text{K}} - I_L, \tag{2.1}$$

$$I_{\text{Na}} = \bar{g}_{\text{Na}} m^3 h (V_m - E_{\text{Na}}), \tag{2.2}$$

$$I_{\text{K}} = \bar{g}_{\text{K}} n^4 (V_m - E_{\text{K}}), \tag{2.3}$$

$$I_L = \bar{g}_L (V_m - E_L). \tag{2.4}$$

Here, C_m is the membrane capacitance, V_m is the neuron membrane potential, I_{ext} is an externally applied current, and $I_{(\cdot)}$, $\bar{g}_{(\cdot)}$, and $E_{(\cdot)}$ are the currents, conductances, and reverse potentials, respectively associated with sodium, potassium, and an ion leak. The gating variables m and h control activation and inactivation of sodium channels, while n controls potassium activation. The gating variables m, h, n are governed by

$$\frac{dx}{dt} = \alpha_x(V_m)(1-x) - \beta_x(V_m)x, \quad x \in \{m, h, n\}, \tag{2.5}$$

with voltage-dependent rates

$$\alpha_m = \frac{0.1(-40 - V_m)}{e^{(-40-V_m)/10} - 1}, \qquad \beta_m = 4e^{-(V_m+65)/18}, \tag{2.6}$$

$$\alpha_h = 0.07e^{-(V_m+65)/20}, \qquad \beta_h = \frac{1}{e^{(-35-V_m)/10} + 1}, \tag{2.7}$$

$$\alpha_n = \frac{0.01(-55 - V_m)}{e^{(-55-V_m)/10} - 1}, \qquad \beta_n = e^{-(V_m+65)/80}/8. \tag{2.8}$$

The typical HH model coefficients are employed: $C_m = 1\,\mu\text{F/cm}^2$, $\bar{g}_{\text{Na}} = 120\,\text{mS/cm}^2$, $\bar{g}_{\text{K}} = 36\,\text{mS/cm}^2$, $\bar{g}_L = 0.3\,\text{mS/cm}^2$, $E_{\text{Na}} = 50\,\text{mV}$, $E_{\text{K}} = -77\,\text{mV}$, $E_L = -54.4\,\text{mV}$.

Our contribution is the introduction of a voltage threshold for spiking, which triggers a reset of the voltage as well as all gating variables. We integrate the HH equations above with the additional condition

$$\text{if } V_m > -35\,\text{mV} \text{ then } \begin{cases} V_m \leftarrow E_{\text{K}}, \\ m \leftarrow 0.0, \\ h \leftarrow -0.27, \\ n \leftarrow 1.08. \end{cases} \tag{2.9}$$

We refer to the use of this additional equation as the hard-reset Hodgkin-Huxley (hrHH) model.

The reset values are chosen by the following logic. The membrane potential after the reset is E_{K} such that $I_{\text{K}} = 0$ as indicated by (2.3), and m is reset to 0 such that $I_{\text{Na}} = 0$ as indicated by (2.2). These currents will remain small as long as the membrane potential remains near the reset value because of (2.3) and because m will remain near zero in this case due to (2.5) and the value of α_m. These conditions imply that shortly after the reset, the evolution of V_m is governed by I_{ext} and I_L, which are typically relatively weak currents and thus reinforce the assumption that the membrane potential remains near the reset voltage for some time after the spike.

The independence of the membrane potential on h and n after the reset allows some freedom in how the reset values of these gating variables are set. The nearly constant membrane potential implies that the evolution of h and n will be fairly independent to the current stimulus and may generalize well for various current stimuli. The values of -0.27 and 1.08 are determined through manual calibration to lead to agreement between the HH and hrHH models response to a current step function. These and other results will be shown in the following chapter.

3 Results

To evaluate the accuracy of the hrHH model in recovering the dynamics of the baseline HH model, we analyze the voltage response of the model to various current stimuli. An analysis of the time evolution of the gating variables, a discussion of why constant reset values seem to generalize well, and preliminary evidence of the impact of the model on numerical stiffness will also be presented in this chapter. For reference, the voltage response of the QSSA and Izh models are also presented. For the former, the original formulation in Hodgkin and Huxley 1952 is used rather than the sigmoid approximation, e.g., used in Rinzel and Ermentrout 1998. For the latter, the coefficients for a “regular spiking" neuron are adopted E. M. Izhikevich 2003. Simulations are performed using the Brian2 simulator Stimberg, Brette, and Goodman 2019 and the following initial values are prescribed: $V_{m,0} = -65\text{mV}, m_0 = 0.05, h_0 = 0.60, n_0 = 0.32$.

In Fig. 1, we consider the models' voltage response to an applied current step function which is 7 μA and turns off at 10 ms. We define the spike-to-trough interval as beginning with the crossing of -35 mV from below and ending with the local minimum voltage occurring after the next local maximum. The hrHH model is designed to avoid resolving the fast dynamics of V_m and m during the spike-to-trough interval; thus, those intervals are shaded in gray to focus attention on the remaining intervals. By construction, the hrHH model registers a spike right at the start of the shaded region. Meanwhile, the QSSA model initiates a spike (exceeds -35 mV) too early the Izh model too late with respect to the HH model. Perhaps surprisingly, the after-trough behavior of the hrHH model almost exactly matches the HH model. The QSSA has only minor errors in this region, and the Izh model is less accurate as it tends towards a resting voltage that is below that of the other models.

In Fig. 2, the response to an applied current of a linear pulse is considered. The applied current linearly increases from 0 to 6 μA from 5 to 8 ms and then returns to zero for the duration. The pulse ends 2 ms before the HH model spike initiates, which makes this case a delayed excitation unlike the prior stimulus considered. Again the hrHH model exactly recovers the HH model dynamics outside of the spike-to-trough interval. For the QSSA model, the spike initiates right after the pulse ends, which leads to an early spike. The Izhikevich model does not spike as the voltage decreases monotonically after the pulse ends indicating an inability to capture the delayed excitation.

In Fig. 3, the response to an applied current of a quadratic pulse is considered. The applied current obeys $I_{ext} = 10t^2/49 - 3$ μA for 14 ms and then is zero for the duration. The hrHH model exactly tracks the voltage of the HH model outside of the spike-to-trough interval. Once again the QSSA model spikes early and the Izh model spikes late. The Izh model also emits two subsequent spurious spikes, the latter of which is a delayed excitation.

3.1 Waveforms and gating variables

Next, the response to two different waveforms is considered to analyze the accumulation of errors in time. Also, time series for the ion gating variables are analyzed to provide additional context on the model dynamics. Since the Izh model has been shown to have different dynamics for a single pulse and does not have gating variables, it is omitted from the following analysis. In Fig. 4, we consider the response to a linear sawtooth waveform current, which linearly increases from 0 to 7 μA over 10 ms and repeats. The HH and hrHH models agree well outside of the spike-to-trough intervals. The QQSA model on the other hand produces two spurious spikes near 20 and 40 ms and misses the spike at 30 ms. This behavior can be explained by examining the gating variable dynamics.

m is the sodium activation channel. QSSA predicts the shape of the rapid rise and fall qualitatively correct, but this happens early, which is consistent with the early spike. For hrHH, the initial rise of m at spike initiation is accurately captured, a spike is registered and m is reset to zero, which roughly corresponds to the after-trough value observed in HH. In this way, the rapid rise and fall of m is bypassed by jumping to the after-trough slow dynamics for which the value of m remains near zero. For the sodium deactivation gating variable h and the potassium activation gating variable n, the early spike in the QSSA model leads to early relaxation of these spike-suppressing variables to their resting (spike-permitting) values, which allows for the spurious spike at 20 ms. For hrHH, the reset values of h and n given in (2.9). These values are just such that it takes the full time until the trough for h and n to relax to the trough values observed with the HH model. This leads to the accurate voltage trajectory for subsequent spikes.

In Fig. 5, a linear pulse waveform current is applied, which linearly increases from 0 to 7 μA over 3 ms, is off for 4 ms, and repeats. The hrHH model correctly predicts that one spike forms shortly after the first linear pulse. The QSSA predicts spurious spikes for every second subsequent pulse. Near the supurious spike initiations, the values

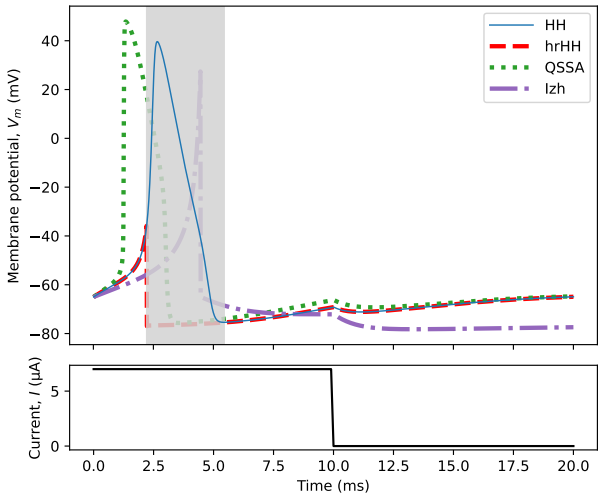

Figure 1. The membrane potential response to a step function applied current for the HH, hrHH, QSSA, and Izh models. The spike-to-trough interval is shaded for the HH reference data.

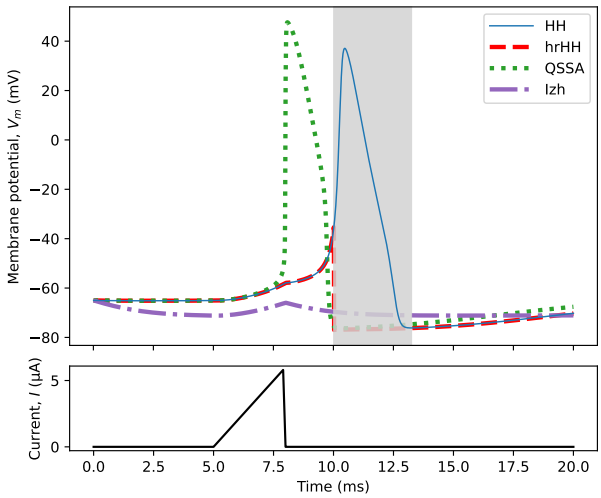

Figure 2. The membrane potential response to a linear pulse applied current for the HH, hrHH, QSSA, and Izh models. The spike-to-trough interval is shaded for the HH reference data.

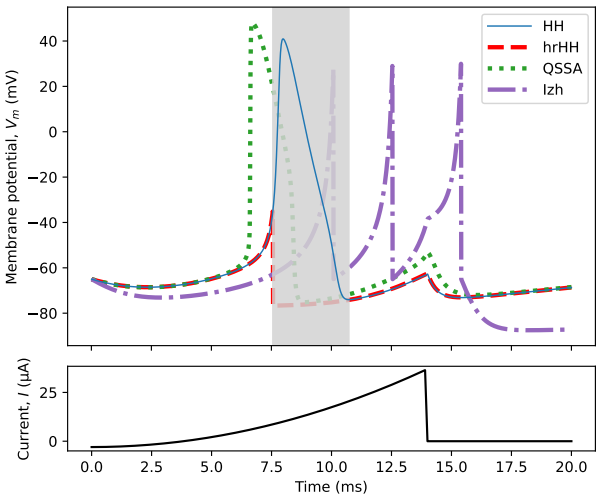

Figure 3. The membrane potential response to a quadratic pulse applied current for the HH, hrHH, QSSA, and Izh models. The spike-to-trough interval is shaded for the HH reference data.

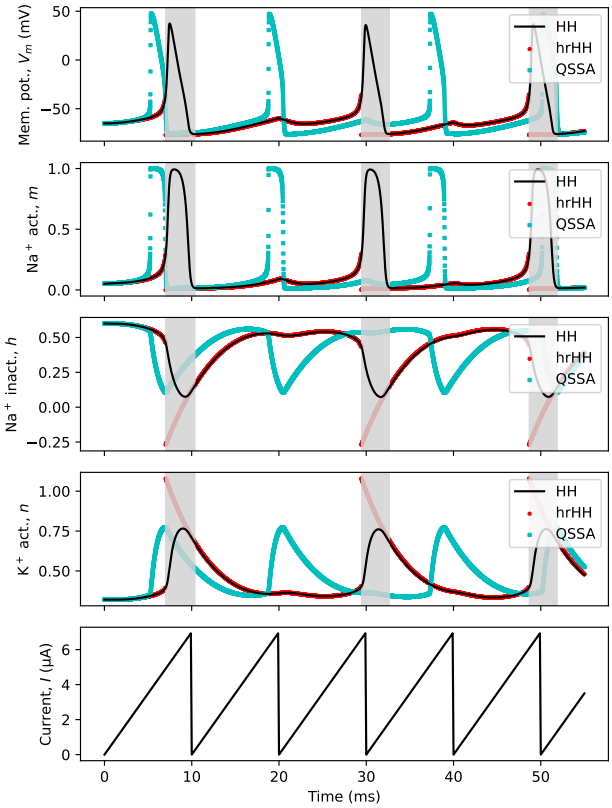

Figure 4. The response of the membrane potential and gating variables to the applied current of a linear sawtooth waveform for the HH, hrHH, and QSSA models. The spike-to-trough intervals are shaded for the HH reference data.

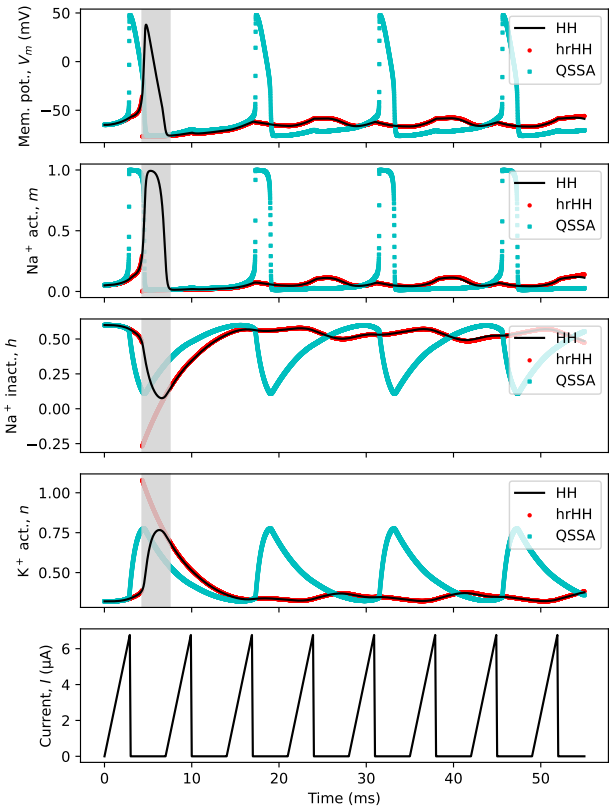

Figure 5. The response of the membrane potential and gating variables to the applied current of a linear pulse waveform for the HH, hrHH, and QSSA models. The spike-to-trough intervals are shaded for the HH reference data.

of m, h, and n are fairly similar across the models, so it is possible that the spurious spikes predicted by the QSSA model are the result of the model's use of an algebraic relation for m_∞ instead of solving the m ODE as in the hrHH or HH models.

It is remarkable that for all of the applied pulses and waveforms considered, the hrHH model, deployed with the hard reset conditions given in (2.9), is accurate outside of the spike-to-trough intervals. To understand why the model is generalizing well without recalibration for different current stimuli, we revisit the assumption made in the model development. Indeed, it is observed that $V_m \approx E_\mathrm{K}$ across the spike-to-trough intervals for all stimuli considered. This implies n and h evolve approximately independently of V_m during these intervals and obey nearly constant coefficient exponential relaxation governing equations (2.5), which have simple dynamics that do not depend on I_ext and essentially track the expiration of the refractory time. Meanwhile, in the HH model, V_m varies rapidly over these intervals (due to rapid variations in m and large $V_m - E_\mathrm{K}$) which leads to relatively complex dynamics for n and h. Since the trough values of n and h are observed to not be varying appreciably between cases with different current stimuli, the simplified dynamics are sufficient to recover these constant trough values through a simple exponential relaxation trajectory as long as predicting the spike-to-trough behavior is not of interest.

As a proxy for quantifying the degree to which the hrHH model reduces the numerical stiffness of the system of equations, without making conclusions that are specific to a particular numerical integration method, the reduction in the maximum membrane potential slope is investigated. For all stimuli considered, the reduction in the maximum slope is between 3.3 and 3.5 times for the hrHH model with respect to the HH model, which implies that the hrHH model avoids the fastest dynamics of the HH model as desired. For the QSSA and Izh models, the slope increases by a factor of 10 and by 10%, respectively, which implies that the dynamics are even faster in these models than in the HH model.

4 Conclusions

The hard reset Hodgkin-Huxley (hrHH) model is proposed. It uses a voltage threshold to detect spikes and resets the voltage and gating variables. The model bypasses the fast time dynamics of spike-to-trough intervals and almost exactly recovers the baseline HH model's voltage and gating variable time series outside of these intervals for all pulses and waveforms considered. The model decreases the maximum voltage slope by a factor between 3.3 to 3.5 with respect to the HH model, which is a proxy for a reduction in numerical stiffness. This suggests that larger time steps could be used when integrating the hrHH model while remaining quantitatively accurate with respect to the HH model outside of spike-to-trough intervals.

References

Hodgkin, A. L., and A. F. Huxley. 1952. “A quantitative description of membrane current and its application to conduction and excitation in nerve.” *J. Physiol.* 117 (4): 500.

Izhikevich, E. 2004. “Which model to use for cortical spiking neurons?” *IEEE Trans. Neural Netw.* 15 (5): 1063–1070. Accessed April 21, 2025. https://doi.org/10.1109/TNN.2004.832719.

Izhikevich, E. M. 2003. “Simple model of spiking neurons.” *IEEE Trans. Neural Netw.* 14 (6): 1569–1572.

Rinzel, J., and G. B. Ermentrout. 1998. “Analysis of neural excitability and oscillations.” In *Methods in neuronal modeling 2,* 251–292.

Stimberg, M., R. Brette, and D. F. Goodman. 2019. “Brian 2, an intuitive and efficient neural simulator.” *elife* 8:e47314.